Nuclear Instruments and Methods in Physics Research A 602 (2009) 687–690

Contents lists available at ScienceDirect

Nuclear Instruments and Methods in Physics Research A

journal homepage: www.elsevier.com/locate/nima

The HADES RPC inner TOF wall

D. Belver [a], A. Blanco [b], P. Cabanelas [a], N. Carolino [b], E. Castro [a], J. Diaz [c], P. Fonte [b,e,*], J.A. Garzón [a], D. Gonzalez-Diaz [d], A. Gil [c], W. Koenig [d], L. Lopes [b], A. Mangiarotti [b], O. Oliveira [b], A. Pereira [b], C. Silva [b], C.C. Sousa [f], M. Zapata [a]

[a] LABCAF-Universidad de Santiago de Compostela, 15782 Santiago de Compostela, Spain
[b] Laboratório de Instrumentação e Física Experimental de Partículas, 3004-516 Coimbra, Portugal
[c] Instituto de Física Corpuscular (CSIC-Universidad de Valencia), Valencia 46071, Spain
[d] Gesellschaft für Schwerionenforschung mbH (GSI), 64291 Darmstadt, Germany
[e] Instituto Superior de Engenharia de Coimbra, 3030-199 Coimbra, Portugal
[f] Escola Superior de Tecnologia e Gestão de Leiria, 2411-901 Leiria, Portugal

ARTICLE INFO

Available online 25 December 2008

Keywords:
HADES
RPC
TOF
Crosstalk
Multi-hit

ABSTRACT

The upgraded HADES inner TOF Wall will cover a total area of 8 m^2 with 1116 variable-geometry 4-gap, symmetric, timing RPCs, readout by 2232 time and charge channels. Each RPC is individually shielded for robust multi-hit performance and optimum use of the readout channels (crosstalk minimization). The double layer configuration provides a useful degree of redundancy for very accurate timing of a large fraction of all particles crossing the detector.

In this paper we describe the concept of the detector, its inner structure and the multi-hit performance.

1. Introduction

The HADES (High-Acceptance DiElectron Spectrometer) at GSI Darmstadt [1], operates in the energy regime of 1–2 AGeV and consists of a 6-coil toroidal magnet centered on the beam axis and six identical detection sections located between the coils and covering polar angles between 18° and 85°. The physics aims include the study of the properties of hot and dense hadronic matter—a key problem in heavy-ion physics—as well as elementary and pion-induced reactions.

For elementary reactions and the study of light systems, up to Ca–Ca, HADES is equipped with a large time-of-flight (TOF) Wall made of plastic scintillator bars readout by photomultipliers. However the multiplicity requirements for the study of larger systems, up to Au–Au, called for an upgraded TOF detector with higher granularity on the inner region, replacing the present TOFINO detector.

The upgraded inner TOF Wall will cover a total area of 8 m^2 with 1116 variable-geometry 4-gap, symmetric, timing RPCs [2], readout by 2232 time and charge channels. The detector is divided in 6 sectors (or sextants) of trapezoidal shape (Fig. 2). Each RPC counter is individually shielded [3] for robust multi-hit performance and optimum use of the readout channels (crosstalk minimization). The double layer configuration provides a useful [4] degree of redundancy for very accurate tail-free timing [5] of a fraction of all particles crossing the detector.

In this communication the concept, construction and some key performance characteristics of the detector will be discussed.

2. Requirements

Taking into consideration the HADES overall performance, the Inner TOF Wall should conform to the following parameters:

- Multi-hit capability: hit-loss probability below 20% for the heaviest system considered;
- Granularity (determined by the multi-hit capability): 150 channels/sector × effective cluster size;
- Resolution: 100 ps σ or better;
- Rate capability: up to 1 kHz/cm^2 in the innermost part;
- Efficiency: above 95% for single hits;
- Area: ~8/6 m^2/sector.

In the above description was introduced the concept of "effective cluster size" that will be further discussed in Section 5.

* Corresponding author at: Laboratório de Instrumentação e Física Experimental de Partículas, 3004-516 Coimbra, Portugal. Tel.: +351 239833465; fax: +351 239822358.
E-mail address: fonte@lipc.fis.uc.pt (P. Fonte).

0168-9002/$ - see front matter © 2008 Elsevier B.V. All rights reserved.
doi:10.1016/j.nima.2008.12.090

3. Detector design

3.1. Prior considerations

Timing RPCs generate signals with bandwidths reaching over 1 GHz [6] and are by necessity readout by electronics with a matching bandwidth. It is clear that in such circumstances signals will be efficiently coupled between neighboring readout electrodes (a capacity of 1 pF has an impedance of only 150 Ω at 1 GHz). This will cause either the triggering of such channels, increasing occupancy (increase that is often defined in terms of a "cluster size"), or baseline shifts that will perturb the correct measurement of time (leading to the "effective cluster size" concept—see the discussion).

The effects are more severe for applications were the optimum electrode size is larger than a few cm^2, calling for long strips readout on both ends by identical time channels. Indeed, a structure composed by parallel conductive strips over a common ground plane is known in microwave engineering as a "microstrip directional *coupler*" [7]. Crosstalk levels up to 80% have been measured on strip-like timing RPCs [8].

For the HADES RPC these issues were tackled by individually shielding each strip [3], at the expense of a somewhat complex mechanics, trying to achieve an effective cluster size close to unity.

3.2. Simulation

The electrical shielding structures, introducing insensitive regions, enforce the use of two staggered layers for full geometric coverage. The inter-layer overlap must be optimized, along with the characteristic change in cell area as a function of polar angle that allows in fixed-target experiments to compensate for the Lorentz boost (Fig. 1).

The more general way to accomplish this [9] is by propagating a distribution that is isotropic and flat in inverse momentum,

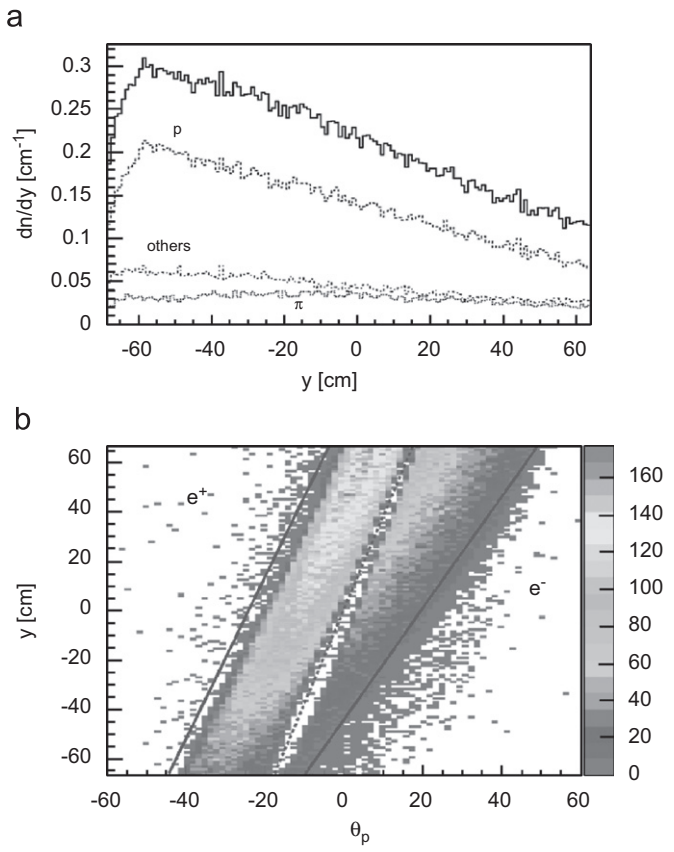

Fig. 1. (a) Distribution of particles along the *y* coordinate (rows direction in Fig. 2) Au–Au central events at 1.5 AGeV. (b) Di-electron spectrum, isotropic and white in inverse momentum, as a function of θ_p (angle projected onto the plane defined by the transverse cross-section of the cell) and *y*.

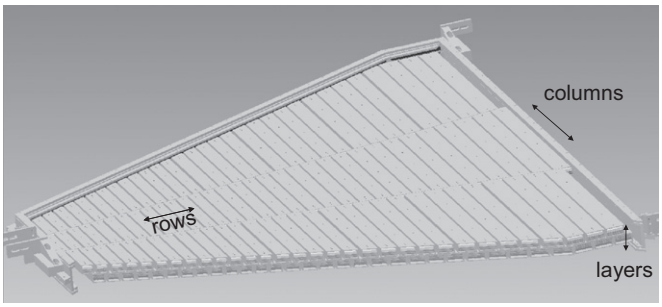

Fig. 2. Drawing of the internal structure of one HADES RPC sector and also parts of the gas box. The detector is composed by individually shielded strip-like counters ("cells"), organized in two partially overlapping layers with 31 rows and 3 columns each. The counters variable width matches the expected local particle density.

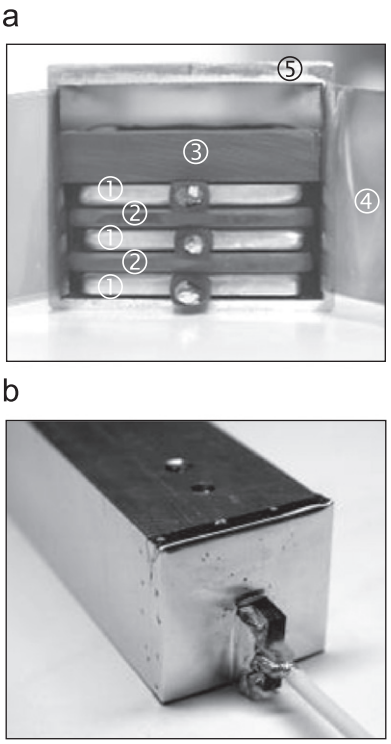

Fig. 3. (a) Internal structure of the cells: 1—Al electrodes; 2—glass electrodes; 3—plastic pressure plate; 4—kapton insulation; 5—2 mm thick Al shielding tube. (b) Finished detector with Al foil shielding end-cap and HV cable.

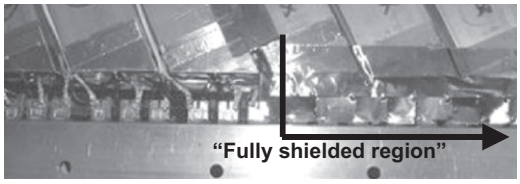

Fig. 4. Detail of the additional copper shielding placed between feedthroughs in rows above # 19. These rows will be called in the text "fully shielded region". Note that all cells are equally shielded: the only difference is this extra copper shielding of about 2 cm length.

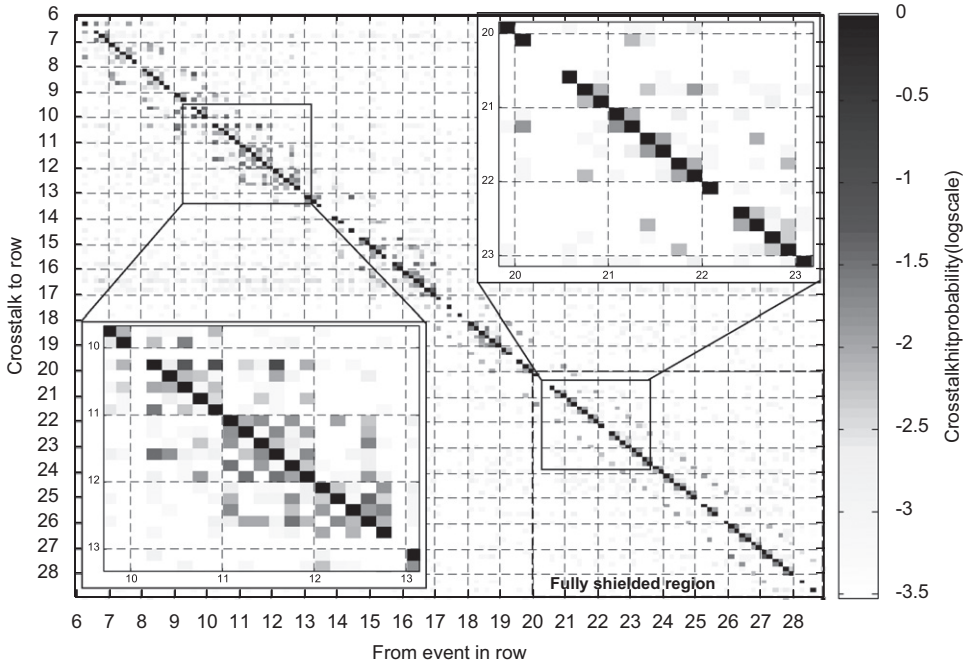

Fig. 5. Crosstalk map between all pairs of cells in the sector. The rows are represented sequentially and there are 6 pixels for each row, representing the columns in that row (see Fig. 2). Columns in one layer are even-numbered while columns in the other layer are odd-numbered. The vertical pixel columns represent the probability that a hit in a given cell (black pixel) will be accompanied by a hit in any other (mind the logarithmic gray scale). Some pixels are missing owing to dead front-end electronic channels. Two regions can be recognized. In the "fully shielded region" (see Fig. 4) crosstalk at the percent level exists mostly to the same row of the opposing layer (the 2×2 square patterns) and a little less to nearby rows also in the opposing layer (the two side bands). There is little crosstalk to the same layer. In the complementary region, crosstalk is widespread amongst all columns in a row on both layers and also to neighboring rows.

being the later proportional in first order to the angle deflected inside a magnetic field. This way, all the possible tracks within the spectrometer are generated with the same weight, allowing to obtain the maximum and minimum angle of incidence over the cell θ_p (angle projected onto the plane defined by the transverse cross-section of the cell) as a function of the y coordinate (defined along the polar angle-rows direction in Fig. 2). The angular range of θ_p for every slice in y (defined by straight lines in Fig. 1) dictates the necessary position of the two immediate neighbors in the opposite plane for providing full geometrical coverage, therefore fixing the overlap as a function of y. To avoid excessively narrow strips, which might be dominated by edge effects, each sector was divided in three columns (Fig. 2), keeping the needed granularity while allowing for wider cells.

Furthermore, for maximizing the potential for the identification of rare particles [4], the overlap was maximized beyond the bounds marked in Fig. 1 until the mechanical limits were reached.

3.3. Counter structure

The detector is composed by individually shielded strip-like RPC counters ("cells"), organized in two partially overlapping layers. Each layer is composed by 31 rows and 3 columns, ranging the widths between 2.2 and 5 cm and the lengths between 12 and 52 cm.

The individual cells are made of 3 aluminum electrodes and 2 glass electrodes, all of 2 mm thickness (Fig. 3). The gap is defined by PEEK[1] monofilaments of 270 μm diameter, spaced between 5 and 10 cm along the cell. The ensemble is housed inside individual shielding tubes and compressed by three springs (not shown) that apply a controlled force to a PVC[2] plate that distributes the force. This arrangement results from an attempt to keep good mechanical uniformity of the gap (any variations above 10% are likely to perturb the time resolution [10]), while minimizing the total glass thickness for optimum count-rate capability.

High-voltage (HV) close to 6 kV is applied to the central electrode via 330 MΩ resistors and high voltage cables, while the outer electrodes are grounded. The glass electrodes are kept electrically floating [11]. Insulation to the shielding tube walls is assured by a triple-layer KAPTON^{TM} adhesive laminate. An end-shield made of aluminum foil is spot-welded on the shielding tubes.

The signals are collected by the HV cable and fed out via a 2 nF coupling capacitor and 50 Ω PCB[3] stripline feedthroughs that cross the lateral wall of the gas box. No attempt is made at detector-cable impedance matching.

The whole sector is made out of heat-resistant materials, chosen to withstand temperatures up to 65 °C without loss of the relevant properties, in case the need for enhanced rate capability [12] arises.

Additional copper shielding is installed between the feed-throughs as shown in Fig. 4. However for this prototype sector such shielding was present only in rows above # 19 to check for its need.

4. Crosstalk and multi-hit performance

A prototype sector was instrumented [13] and tested in beam as described in [14]. In here we will discuss only its multi-hit performance.

A map of crosstalk hits between all pairs of cells in the sector is shown in Fig. 5. A crosstalk hit is defined as a hit that shows a

[1] Polyetheretherketone.
[2] Polyvinyl chloride.
[3] Printed circuit board.

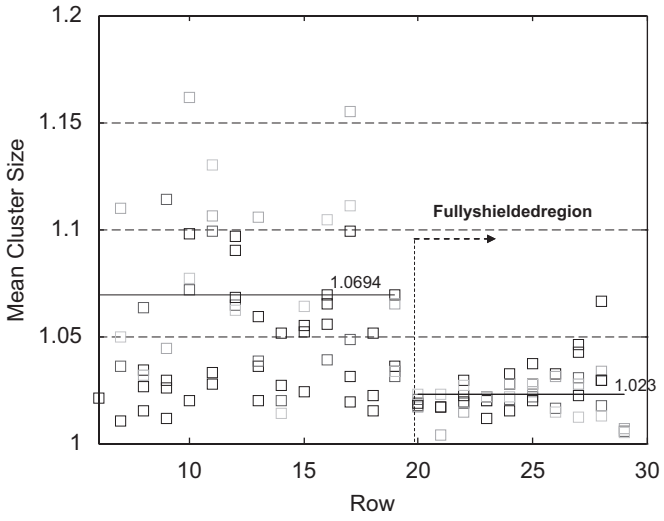

Fig. 6. The average cluster size—average number of cells fired per event—for events containing only one good hit. There is a small but clear difference between the "fully shielded region" (1.023) and the rest of the detector (1.069).

physically impossible longitudinal position along the cell (determined by the time difference between the cell ends) and a charge measurement compatible with zero. Naturally, a crosstalk hit must be accompanied by a single good hit somewhere in the detector. Only events with a single good hit were considered for the crosstalk study.

There are clear patterns (Fig. 5) showing that the little extra shielding placed between the signal feedthroughs as shown in Fig. 4 reduces crosstalk in a visible way. It is clear that if the cells themselves wouldn't be shielded disastrous crosstalk levels would occur [9].

Fig. 6 shows the average cluster size—average number of cells fired per event—for events containing only one good hit: 1.023 (2.3% crosstalk) in the "fully shielded region" (see Fig. 4), while in the complementary region the mean cluster size noticeably increases to 1.069 (6.9% crosstalk).

5. Discussion

It remains the question whether the little difference in crosstalk performance evidenced in Fig. 6 may have any visible impact on the detector performance. Indeed, it does, as it can be seen in [14]. The "fully shielded region", however small the extra shielding is, shows a slightly better time resolution and less dispersion of the time resolution values. The same pattern can be seen on the position resolution data, which relies also on time measurements. This cannot be directly ascribed to the excess of hits caused by crosstalk, but to the baseline shifts that, even at sub-threshold level, will still cause an erroneous measurement of time.

Therefore it seems clear that for timing RPCs the usual "cluster size" concept used to represent the amount of crosstalk in detectors has to be extended to an "effective cluster size", which will represent the number of channels in the neighborhood of a hit whose time would be affected if a particle would cross them. This is likely quite difficult to measure and depends, for instance, on the charge and time relations between the hit pair.

6. Conclusion

The upgraded inner TOF Wall will cover a total area of 8 m^2 with 1116 variable-geometry 4-gap, symmetric, timing RPCs, readout by 2232 time and charge channels. The detector is divided in 6 sectors (or sextants) of trapezoidal shape. Each RPC counter is individually shielded for robust multi-hit performance and optimum use of the readout channels (crosstalk minimization). The double layer configuration provides a useful degree of redundancy for very accurate tail-free timing of a fraction of all particles crossing the detector.

Beam tests yielded a small but clear difference in average cluster size between the "fully shielded region" (2.3% crosstalk) and the rest of the detector (6.9% crosstalk), which lacks a mere 2 cm copper foil shielding between the signal feedout connectors (see Fig. 4). More significantly, it was measured [14] a small but consistent difference of the time and position resolutions between both regions, along with a smaller dispersion of the values in the "full-shielded region".

The results show that crosstalk was very thoroughly suppressed, but that even very minor shielding faults may have noticeable impact on timing performance.

Acknowledgments

We thank the important contributions of I. Koenig, S. Lange, G. May, J. Markert, M. Palka, J. Pietraszko, E. Schwab, M. Traxler, R. Trebacz and the GSI nuclear electronics group.

This work was co-financed by FCT, EU, FEDER and POCI via the contract POCI/FP/81982/2007, the EU 6th Framework Program under contracts RII3-CT-2004-506078 and RII3-CT-2005-515876, the INTAS project 06-1000012-8861, by MEC under grants FPA2006-09154 and FPA2006-12120-C03-02 and by XUGA under grant PGIDIT06PXIC20601PM.

References

[1] P. Salabura, et al., Nucl. Phys. A 749 (2005) 150.
[2] P. Fonte, A. Smirnitski, M.C.S. Williams, Nucl. Instr. and Meth. A 443 (2000) 201.
[3] C. Finck, et al., Nucl. Instr. and Meth. A 508 (2003) 63–69.
[4] A. Mangiarotti, et al., Nucl. Instr. and Meth. A (2009), doi:10.1016/j.nima.2008.12.139.
[5] A. Blanco, et al., PoS(HEP2005) 376.
[6] A. Blanco, et al., IEEE Trans. Nucl. Sci. 48 (4) (2001) 1249–1253.
[7] D.M. Pozar, Microwave Engineering, Wiley, New York, ISBN 978-0471448785, 2004.
[8] A. Blanco, et al., Nucl. Instr. and Meth. A 485 (2002) 328–342.
[9] D. Gonzalez-Diaz, Ph.D. thesis, Universidade de Santiago de Compostela, Spain (2006) 〈http://jinst.sissa.it/jinst/theses/2006_JINST_TH_003.pdf〉.
[10] A. Blanco, et al., Nucl. Instr. and Meth. A 535 (2004) 272–276.
[11] E. Cerron Zeballos, et al., Nucl. Instr. and Meth. A 374 (1976) 132–135.
[12] D. Gonzalez-Diaz, et al., Nucl. Instr. and Meth. A 555 (2005) 72–79.
[13] D. Belver, et al., Nucl. Instr. and Meth. A (2009), doi:10.1016/j.nima.2008.12.135.
[14] D. Belver, et al., In-beam measurements of the HADES-TOF RPC wall, these proceedings.